

University of Groningen

## PI3K inhibition reduces murine and human liver fibrogenesis in precisioncut liver slices

Gore, Emilia; Bigaeva, Emilia; Oldenburger, Anouk; Ook, Kim Yong; Rippmann, Jörg F; Schuppan, Detlef; Boersema, Miriam; Olinga, Peter

*Published in:*  
Biochemical Pharmacology

*DOI:*  
[10.1016/j.bcp.2019.113633](https://doi.org/10.1016/j.bcp.2019.113633)

**IMPORTANT NOTE: You are advised to consult the publisher's version (publisher's PDF) if you wish to cite from it. Please check the document version below.**

*Document Version*  
Publisher's PDF, also known as Version of record

*Publication date:*  
2019

[Link to publication in University of Groningen/UMCG research database](#)

*Citation for published version (APA):*

Gore, E., Bigaeva, E., Oldenburger, A., Ook, K. Y., Rippmann, J. F., Schuppan, D., Boersema, M., & Olinga, P. (2019). PI3K inhibition reduces murine and human liver fibrogenesis in precisioncut liver slices. *Biochemical Pharmacology*, 169, [113633]. <https://doi.org/10.1016/j.bcp.2019.113633>

### Copyright

Other than for strictly personal use, it is not permitted to download or to forward/distribute the text or part of it without the consent of the author(s) and/or copyright holder(s), unless the work is under an open content license (like Creative Commons).

The publication may also be distributed here under the terms of Article 25fa of the Dutch Copyright Act, indicated by the "Taverne" license. More information can be found on the University of Groningen website: <https://www.rug.nl/library/open-access/self-archiving-pure/taverne-amendment>.

### Take-down policy

If you believe that this document breaches copyright please contact us providing details, and we will remove access to the work immediately and investigate your claim.

*Downloaded from the University of Groningen/UMCG research database (Pure): <http://www.rug.nl/research/portal>. For technical reasons the number of authors shown on this cover page is limited to 10 maximum.*



ELSEVIER

Contents lists available at ScienceDirect

## Biochemical Pharmacology

journal homepage: [www.elsevier.com/locate/biochempharm](http://www.elsevier.com/locate/biochempharm)

## PI3K inhibition reduces murine and human liver fibrogenesis in precision-cut liver slices



Emilia Gore<sup>a</sup>, Emilia Bigaeva<sup>a</sup>, Anouk Oldenburger<sup>b</sup>, Yong Ook Kim<sup>c</sup>, Jörg F. Rippmann<sup>b</sup>, Detlef Schuppan<sup>c,d</sup>, Miriam Boersema<sup>a,1</sup>, Peter Olinga<sup>a,\*,1</sup>

<sup>a</sup> Groningen Research Institute of Pharmacy, Department of Pharmaceutical Technology and Biopharmacy, University of Groningen, Antonius Deusinglaan 1, Groningen 9713AV, The Netherlands

<sup>b</sup> Cardiometabolic Disease Research, Boehringer Ingelheim Pharma GmbH & Co. KG, Birkendorfer Str. 65, Biberach an der Riss 88397, Germany

<sup>c</sup> Institute of Translational Immunology and Research Center for Immunotherapy, University Medical Center, Johannes Gutenberg University, Obere Zahlbacherstraße 63, Mainz 55131, Germany

<sup>d</sup> Division of Gastroenterology, Beth Israel Deaconess Medical Center, Harvard Medical School, Boston, 330 Brookline Avenue, MA 02215, USA

## ARTICLE INFO

## Keywords:

Precision-cut tissue slices  
Liver fibrosis  
Ompalisib  
PI3K  
Jejunum

## ABSTRACT

**Background:** Liver fibrosis results from continuous inflammation and injury. Despite its high prevalence worldwide, no approved antifibrotic therapies exist. Ompalisib is a selective inhibitor of the PI3K/mTOR pathway that controls nutrient metabolism, growth and proliferation. It has shown antifibrotic properties *in vitro*. While clinical trials for idiopathic pulmonary fibrosis have been initiated, an in-depth preclinical evaluation is lacking. We evaluated ompalisib's effects on fibrogenesis using the *ex vivo* model of murine and human precision-cut tissue slices (PCTS).

**Methods:** Murine and human liver and jejunum PCTS were incubated with ompalisib up to 10  $\mu\text{M}$  for 48 h. PI3K pathway activation was assessed through protein kinase B (Akt) phosphorylation and antifibrotic efficacy was determined via a spectrum of fibrosis markers at the transcriptional and translational level.

**Results:** During incubation of PCTS the PI3K pathway was activated and incubation with ompalisib prevented Akt phosphorylation ( $\text{IC}_{50} = 20$  and 1.5 nM for mouse and human, respectively). Viability of mouse and human liver PCTS was compromised only at the high concentration of 10 and 1–5  $\mu\text{M}$ , respectively. However, viability of jejunum PCTS decreased with 0.1 (mouse) and 0.01  $\mu\text{M}$  (human). Spontaneously increased fibrosis related genes and proteins were significantly and similarly suppressed in mouse and in human liver PCTS.

**Conclusions:** Ompalisib has antifibrotic properties in *ex vivo* mouse and human liver PCTS, but higher concentrations showed toxicity in jejunum PCTS. While the PI3K/mTOR pathway appears to be a promising target for the treatment of liver fibrosis, PCTS revealed likely side effects in the intestine at higher doses.

### 1. Introduction

Liver fibrosis is a chronic disease caused by continuous injury, with a high prevalence worldwide. Liver injury can be caused by different factors, such as viruses, alcohol, hepatotoxic compounds, and metabolic disorders [3,32]. Chronic injury causes liver damage and leads to the replacement of functional tissue with extracellular matrix (scarring/fibrosis) [31]. Liver fibrosis has a quiet and gradual pathology, which can evolve to cirrhosis during years to decades. When the primary causal factor is removed, even advanced fibrosis can reverse, whereas cirrhosis is generally regarded as irreversible [28,35].

Various pathways, mediators and cells modulate the progression of liver fibrosis [30]. A key player in this fibrogenesis process is the activated hepatic stellate cell (HSC) and related myofibroblasts (MF). As a result of chronic liver damage, HSC lose their physiological role of vitamin A storage, and differentiate into extracellular matrix secreting MF [20]. Furthermore, activated HSC/MF show increased proliferation, migration, contractility and apoptosis resistance [1]. These cellular processes are modulated by different growth factors (platelet-derived growth factor (PDGF), transforming growth factor beta (TGF $\beta$ ), epidermal growth factor (EGF), vascular endothelial growth factor (VEGF), basic fibroblast growth factor (bFGF), which can all activate the

\* Corresponding author at: University of Groningen, Department of Pharmaceutical Technology and Biopharmacy, Antonius Deusinglaan 1, 9713AV Groningen, The Netherlands.

E-mail address: [p.olinga@rug.nl](mailto:p.olinga@rug.nl) (P. Olinga).

<sup>1</sup> Shared last authorship.

<https://doi.org/10.1016/j.bcp.2019.113633>

Received 27 June 2019; Accepted 3 September 2019

Available online 05 September 2019

0006-2952/ © 2019 The Author(s). Published by Elsevier Inc. This is an open access article under the CC BY license

(<http://creativecommons.org/licenses/by/4.0/>).

Phosphatidylinositol 3-kinase (PI3K) – protein kinase B (Akt) signaling cascade.

The PI3K family consists of three classes, with Class I PI3K being the best studied, since it is the only one that can produce phosphatidylinositol (3,4,5)-trisphosphate [14], an essential messenger involved in the activation of the downstream signaling. Class I PI3Ks are heterodimeric enzymes that have a catalytic (p110 $\alpha$ ,  $\beta$ ,  $\delta$  or  $\gamma$ ) and a regulatory subunit [14]. The pathway is activated as a response to numerous stimuli and regulates several cellular functions, such as cell survival, proliferation and energy metabolism. As a result, the PI3K pathway is emerging as a promising therapeutic target and is currently studied as a target for several conditions, such as autoimmune rheumatic diseases [2], idiopathic pulmonary fibrosis (IPF) [23], malignancies [41] and liver fibrosis [33]. The latter study showed that HS-173, a PI3K p110 $\alpha$  inhibitor, suppressed cell proliferation and collagen synthesis in hepatic stellate cells [33].

Several Class I PI3K inhibitors were developed and are currently investigated in preclinical or clinical studies. These compounds include pan-isoform inhibitors, which can inhibit all four catalytic isoforms of Class I PI3K, and isoform-specific inhibitors [34]. Although these compounds show promising results and can be fairly well tolerated in patients, there are toxic side effects that have to be taken into account. The most frequent side effects encountered in oncologic patients are hyperglycemia, skin toxicity and gastrointestinal problems [6].

In the current investigation, we evaluated the toxicity and anti-fibrotic effect of a Class I PI3K pan-inhibitor of the catalytic subunit, omipalisib (GSK2126458, GSK458), in murine and human *ex vivo* precision-cut tissue slices (PCTS), a model for early onset and end stage of fibrosis, with human PCTS serving as a bridge towards human studies.

## 2. Methods and materials

### 2.1. Chemicals

Omipalisib (GSK2126458, GSK458) was purchased from Selleckchem (Munich, Germany). The 5 mM stock solution was prepared by dissolving omipalisib in DMSO (Sigma-Aldrich, Saint Louis, MO, USA) and it was stored at  $-80^{\circ}\text{C}$ . The stock solution was diluted in culture media with a final DMSO concentration  $\leq 0.4\%$ .

### 2.2. Ethics statements

This study was approved by the Medical Ethical Committee of the University Medical Centre Groningen, according to Dutch legislation and the Code of Conduct for dealing responsibly with human tissue in the context of health research ([www.federa.org](http://www.federa.org)), refraining the need of written consent for ‘further use’ of coded-anonymous human tissue.

The animal experiments were approved by the Animal Ethics Committee of the University of Groningen (DEC 6416AA-001) and by the Animal Care and Use Committee of the State of Rhineland Palatinate (approval No. 2317707/G12-1-007) and Baden-Württemberg (approval No. 13-011-G), Germany.

### 2.3. Human tissue

Human tissue was obtained from surgical excess material of patients with different pathologies. Clinically healthy liver tissue was acquired from donors undergoing partial hepatectomy or organ donation. Cirrhotic liver tissue originated from patients with end-stage liver disease who underwent liver transplantation. Clinically healthy jejunum tissue was obtained from patients who had a pancreaticoduodenectomy procedure.

### 2.4. Animal care and use statement

The used protocol was designed to minimize animal pain and

discomfort. All mice were housed in a specific pathogen free facility on a 12 h light/dark cycle, with controlled temperature and humidity. Chow and water consumption was ad libitum. All mice were sacrificed under isoflurane (Nicholas Piramal, London, UK) anesthesia by cervical dislocation or exsanguination.

### 2.5. Mouse tissue – liver and jejunum

Adult male 8 week-old C57BL/6 (BL/6) were obtained from Centrale Dienst Proefdieren, UMCG, Groningen, The Netherlands, and male and female 9-week-old FVB mice were purchased from Janvier Labs (Le Genest-Saint-Isle, France). Adult male and female, 9 week-old, Mdr2(abcb4)  $-/-$  mice (FVB background) were bred at the Institute of Translational Immunology at Mainz, Germany and have previously been characterized [27,26]. FVB mice served as controls. Male BL/6 mice (8 weeks of age, purchased from Janvier Labs) were placed on a choline deficient L-amino acid (CDAA, E15666-94, Ssniff Spezialdiäten GmbH, Soest, Germany) defined diet to produce nonalcoholic steatohepatitis or a choline supplemented L-amino acid defined control diet (CSAA, E15668-04, Ssniff Spezialdiäten GmbH) for 12 weeks.

After sacrifice, the livers were collected in cold University of Wisconsin (UW) preservation solution (DuPont Critical Care, Waukegan, IL, USA) and kept on ice until liver PCTS were prepared. The jejunum was collected only from naïve BL/6 mice and preserved in ice-cold Krebs-Henseleit buffer supplemented with 25 mM D-glucose (Merck, Darmstadt, Germany), 25 mM NaHCO<sub>3</sub> (Merck), 10 mM HEPES (MP Biomedicals, Aurora, OH, USA), saturated with carbogen (95% O<sub>2</sub>/5% CO<sub>2</sub>) and pH 7.42 until jejunum PCTS were prepared.

### 2.6. Preparation of precision-cut tissue slices

PCTS from liver and jejunum were prepared as previously described [9], using the Krumdieck tissue slicer (Alabama Research and Development, Munford, AL, USA). Liver PCTS (diameter 5 mm, thickness 250–300  $\mu\text{m}$ , weight 4–5 mg) and jejunum PCTS (thickness 300–400  $\mu\text{m}$ , weight 3–4 mg) were incubated for 48 h with different concentrations of omipalisib or solvent control (DMSO; solvent concentration  $\leq 0.4\%$ ). Liver PCTS and human jejunum PCTS were incubated individually in 12-well plates containing 1.3 ml of Williams Medium E (with L glutamine, Invitrogen, Paisley, Scotland) supplemented with 25 mM glucose, 50  $\mu\text{g}/\text{ml}$  gentamycin (Invitrogen) and exclusively for jejunum PCTS 2.5  $\mu\text{g}/\text{mL}$  amphotericin-B (Invitrogen). Mouse jejunum PCTS were incubated in 24-well plates containing 0.5 ml medium with the same composition as for human jejunum PCTS. Fig. 1 is a schematic representation of the tissues used for the experiments. The slices were cultured under the following conditions:  $37^{\circ}\text{C}$ , 75–90% O<sub>2</sub> and 5% CO<sub>2</sub>, horizontally shaken at 90 rpm. The PCTS culture medium containing drug or solvent was changed after 24 h incubation.

### 2.7. Viability of PCTS

To assess the viability of PCTS, we determined the amount of adenosine triphosphate (ATP) using a bioluminescence kit (Roche, Mannheim, Germany). The obtained ATP value (pmol) was normalized to the total protein content ( $\mu\text{g}$ ), which was evaluated with the Lowry method (RC DC Protein Assay, Bio Rad, Veenendaal, The Netherlands). The results are presented as relative values of the treated groups compared to control.

### 2.8. Gene expression analysis

We performed quantitative reverse transcription polymerase chain reaction (qRT-PCR) in order to assess the gene expression of several fibrosis-related markers. We extracted total RNA from pooled snap-frozen PCTS (liver-3 slices, jejunum-6 slices), using the FavorPrep™

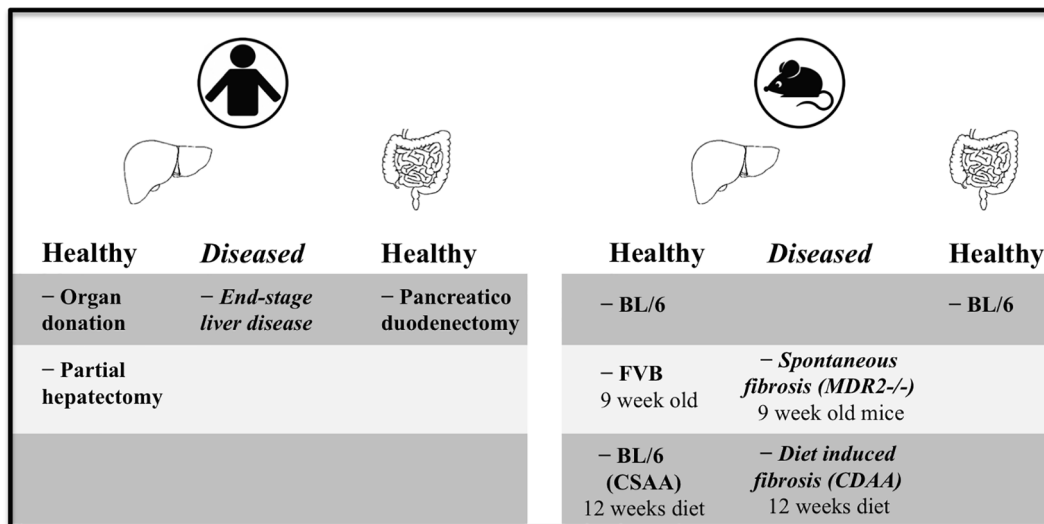


Fig. 1. Schematic representation of the tissues used for the experiments.

Tissue Total RNA Mini Kit (Favorgen, Vienna, Austria). The quantity and quality of extracted RNA was assessed using the BioTek Synergy HT (BioTek Instruments, Winooski, VT, USA). Next, 1 µg total RNA was reverse transcribed to cDNA using the Reverse Transcription System (Promega, Leiden, The Netherlands) using the following protocol: 22 °C for 10 min (min), 42 °C for 15 min and 95 °C for 5 min. qRT-PCR was performed in a ViiA 7 Real-Time PCR System (Applied Biosystems, Bleiswijk, The Netherlands) using SYBR Green (Roche) or TaqMan (Roche) based detection (with 1 cycle of 10 min 95 °C and 40 cycles of 15 s(s) 95 °C, 30 s 60 °C and 30 s 72 °C for SYBR Green and 1 cycle of 10 min 95 °C and 40 cycles of 15 s 95 °C, 60 s 60 °C for TaqMan). The gene expression of several fibrosis markers was determined using the Double Delta Ct analysis, with *Actb*, *Gapdh*, *Hmbs* (murine) or *GAPDH* (human) as reference gene. Healthy BL/6 liver PCTS were analyzed using *Actb*; for *Mdr2*<sup>-/-</sup>, FVB liver PCTS and BL/6 jejunum PCTS *Gapdh* was used, while liver PCTS obtained from mice on CDAA and CSAA diets were analyzed using *Hmbs*. All human samples PCTS were analyzed using *GAPDH*. We detected and excluded significant outliers with the Grubbs' test (significance level alpha = 0.01). The results show the fold induction of each gene ( $2^{-\Delta\Delta Ct}$ ). The primer sequences used in this study are presented in Table 1 (mouse) and Table 2 (human).

## 2.9. Western blotting

Western blotting was used to assess phosphorylated Akt, a downstream protein kinase of the PI3K pathway. For this measurement, three slices were pooled, snap frozen in liquid nitrogen and stored at 80 °C until analysis. The samples were lysed in Ripa buffer (Thermo Scientific, Rockford, IL, USA) containing protease inhibitor cocktail (Sigma-Aldrich) and phosphatase inhibitor (Roche, Mannheim, Germany). 100 µg of proteins were separated with SDS-PAGE using 10% polyacrylamide gels containing 2,2,2-trichloroethanol (Sigma-

Table 2

Taqman gene expression assay for human PCTS.

Gene	Name	Taqman assay
<i>GAPDH</i>	Glyceraldehyde-3-phosphate dehydrogenase	Hs02758991_g1
<i>COL1A1</i>	Collagen, type I, alpha 1	Hs00164004_m1
<i>SERPINH1</i>	Serine (or cysteine) peptidase inhibitor, clade H, member 1	Hs01060397_g1
<i>ACTA2</i>	Actin, alpha 2, smooth muscle, aorta	Hs00426835_g1
<i>FN1</i>	Fibronectin 1	Hs01549976_m1

Aldrich) for total protein quantification and transferred to a polyvinylidene difluoride membrane using the Trans-Blot® Turbo™ Transfer System according to the protocols of the manufacturer (Bio-Rad). The membranes were blocked with 5% nonfat dry milk in TBST, incubated with primary antibody (rabbit anti-phospho-Akt (Ser473) #9271 or rabbit anti-Akt #9272, Cell Signaling, Leiden, The Netherlands) overnight, washed, incubated with a secondary antibody (Goat anti-rabbit, GARPO, Dako, Glostrup, Denmark) and washed again. Visualization of targeted proteins was done with the Clarity Western ECL Substrate (Bio-Rad) using the ChemiDoc Touch Imaging System (Bio-Rad). Signal intensity was processed using Image Lab™ Software (Bio-Rad). Normalization of the chemiluminescent blot was done using total lane protein. The results are presented as relative values of the treated groups compared to control.

## 2.10. Hydroxyproline analysis

We determined hepatic hydroxyproline (hyp) from 110 to 150 mg FVB liver, 65–85 mg *Mdr2*<sup>-/-</sup> liver and 260–350 mg liver from mice on CDAA and CSAA diets. The tissue was hydrolyzed in a 6 N solution of HCl (Merck) overnight at 110 °C (volume solution: 100 µL for FVB, 500

Table 1

SYBR Green primer sequences used for murine PCTS.

Gene	Name	Forward	Reverse
<i>Actb</i>	Actin, beta	ATCGTGCCTGACATCAAAGA	ATGCCACAGGATTCATACC
<i>Gapdh</i>	Glyceraldehyde-3-phosphate dehydrogenase	ACAGTCCATGCCATCACTGC	GATCCACGACGGACACATTG
<i>Hmbs</i>	Hydroxymethylbilane synthase	ATGAGGGTGATTGCGAGTGGG	TTGTCTCCCGTGGTGGACATA
<i>Col1a1</i>	Collagen, type I, alpha 1	TGACTGGAAGAGCGGCGAGT	ATCCATCGGTCATGCTCTCT
<i>Serpinh1</i>	Serine (or cysteine) peptidase inhibitor, clade H, member 1	AGGTACCAAGGATGTGGAG	CAGCTTCTCCTTCTCGTGT
<i>Acta2</i>	Actin, alpha 2, smooth muscle, aorta	ACTACTGCCGAGCGTGAGAT	CCAATGAAAGATGGCTGGAA
<i>Fn1</i>	Fibronectin 1	CGGAGAGAGTGCCCTACTA	CGATATTGGTGAATCGCAGA



uL for *Mdr2*<sup>-/-</sup>, and 5 ml for CDAA and CSAA). We diluted the samples in citric-acetate buffer and treated them with Chloramine T (Sigma-Aldrich) and 4-(dimethyl)aminobenzaldehyde (Sigma-Aldrich). We measured the absorbance of the samples was measured at 550 nm. The results are presented as  $\mu\text{g}$  hepatic hyp/mg tissue.

### 2.11. Human Pro-Collagen I $\alpha 1$

We measured the content of human Pro-Collagen I  $\alpha 1$  in the incubation media of human liver PCTS using an ELISA kit (DY6220-05, R & D Systems, Abingdon, UK). The determination was performed on media pooled from three slices from the same group and it was done according to the manufacturer's protocol. The results were calculated using a second order polynomial (quadratic) regression for the standard curve and they represent the relative values of the treated groups compared to control or the average concentration of Pro-Collagen I  $\alpha 1$  (pg/ml).

### 2.12. Histopathological analysis

Formalin-fixed, paraffin-embedded PCTS 4- $\mu\text{m}$  sections were stained with hematoxylin and eosin (H&E) for morphology and Picro sirius red (SR) for fibrosis. The images were acquired with NanoZoomer S360 (Hamamatsu, Hamamatsu, Japan).

### 2.13. Data and statistical analysis

We used 3 to 10 different organs for experiments, using triplicate slices for all measurements. The results are expressed as mean  $\pm$  standard error of the mean (SEM). Significance was established using Student's *t*-test or ANOVA and Dunnett's multiple comparison test, with significance  $p < 0.05$ , using the GraphPad Prism 6.0 software.

## 3. Results

### 3.1. Omipalisib inhibits the activation of the PI3K pathway in liver PCTS

To determine the activity of the PI3K pathway in murine liver PCTS, we evaluated PI3K activation through the phosphorylation of its downstream signaling protein – Akt. We assessed pAkt by Western blot before and after 30', 1 h, 2 h and 48 h of incubation in liver PCTS. The PI3K pathway was activated during culture (Fig. 2). Phosphorylation increased in the first hour of incubation and decreased afterwards, but Akt phosphorylation at the end of the incubation time (48 h) was higher than after the first hour. Omipalisib 1  $\mu\text{M}$  inhibited the phosphorylation at every tested time point. Differences were observed also for total Akt, as this protein increased during culture only in the untreated slices. Therefore, the PI3K pathway is activated during culture in liver PCTS and omipalisib can inhibit PI3K activation.

The inhibitory constants of omipalisib for all isoforms were previously assessed in cell-free assays and are in the picomolar range [18]. To determine the concentration of omipalisib that will result in a 50% decrease of Akt phosphorylation in PCTS ( $\text{IC}_{50}$ ), we incubated BL/6 mouse and human liver PCTS with 0.1 nM to 100 nM omipalisib for 1 h. The  $\text{IC}_{50}$  of omipalisib was 20 nM for BL/6 liver PCTS, while lower concentrations were necessary for human liver PCTS – 1.7 nM (healthy) and 2.9 nM (fibrotic) (Fig. 3). The concentrations needed for *ex vivo* PCTS are  $10^2$ - $10^3$  higher compared to a cell-free assay [18].

### 3.2. Omipalisib reduces fibrosis markers in murine and human liver PCTS

#### 3.2.1. Healthy BL/6 liver PCTS

To evaluate the antifibrotic effect of omipalisib and its toxicity in liver, we tested three concentrations (0.1, 1 and 10  $\mu\text{M}$ ) in PCTS from healthy livers from BL/6 mice, based on the  $\text{IC}_{50}$  results (Fig. 3), the half-life of 2 h and high selectivity (more than 10,000 fold compared to

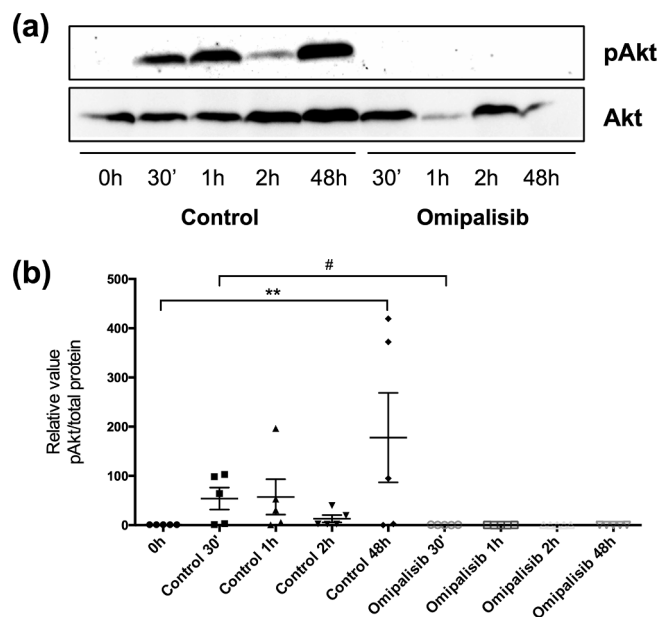


Fig. 2. Time dependent Akt phosphorylation during BL/6 liver PCTS 48 h culture. (a) Representative immunoblot for five experiments where liver PCTS were treated with 0.04% DMSO (control) or omipalisib 1  $\mu\text{M}$  and phosphorylated Akt and total Akt were assessed via WB. (b) Average protein expression of phosphorylated Akt in liver PCTS that were incubated with solvent (0.04% DMSO) or omipalisib 1  $\mu\text{M}$ . Data represents means  $\pm$  SEM of all experimental groups after normalization to total protein; \*\* $p < 0.01$  significantly different from 0 h control; #  $p < 0.05$  significantly different from control at the same time point;  $n = 5$ .

other kinases, except mTOR, a class IV PI3K protein kinase) [18]. First, we assessed the effect of omipalisib on ATP content. Incubation of liver PCTS with omipalisib up to 1  $\mu\text{M}$  for 48 h did not decrease ATP content (Fig. 4a). At 10  $\mu\text{M}$ , however, ATP content was decreased by 20% compared to the control.

We then evaluated the antifibrotic effect of omipalisib on the gene expression level. Previous work showed that slicing and incubation of healthy rat [38] and human [37] liver PCTS induces fibrogenesis, making this system a model of early onset of fibrosis. Omipalisib induced a dose dependent decrease of *Col1a1*, 47 kDa heat shock protein (*Serpinh1*) and *Fn1* (Fig. 4b). 0.1  $\mu\text{M}$  showed only a trend in decreasing the expression of *Col1a1* and had no effect on the other two markers. At 1  $\mu\text{M}$  *Col1a1* and *Serpinh1* were significantly decreased, and at 10  $\mu\text{M}$  all three markers were significantly suppressed. The drug did not affect the expression of the myofibroblast activation marker *Acta2*. Thus, in mouse liver PCTS, omipalisib exerted a clear antifibrotic effect at 1  $\mu\text{M}$ .

#### 3.2.2. Fibrotic *Mdr2*<sup>-/-</sup> liver PCTS

The next step was to evaluate omipalisib in diseased, i.e., fibrotic livers. To this aim we studied the drug in two models of murine liver fibrosis. Here PCTS represent a model of end-stage fibrosis, due to further increase in gene expression of fibrosis markers during incubation.

*Mdr2*<sup>-/-</sup> mice (FVB background) develop spontaneous biliary fibrosis after birth [26]. The SR staining (Fig. 5a) and a 2.2 fold increase in hepatic hyp content compared to FVB mice (Fig. 5b) confirm the presence of liver fibrosis in *Mdr2*<sup>-/-</sup> mice prior to PCTS incubation. At age 9 weeks the *Mdr2*<sup>-/-</sup> and FVB mice show a clear difference regarding fibrosis markers, with *Col1a1*, *Serpinh1* and *Fn1* being highly upregulated (Fig. 5c), while *Acta2* was increased 2.5-fold (not significant). In *Mdr2*<sup>-/-</sup> and FVB control liver PCTS, two omipalisib concentrations, 1 and 5  $\mu\text{M}$ , were tested, based on proven viability and antifibrotic results in PCTS of healthy BL/6 mice. These concentrations did not affect the ATP levels of the *Mdr2*<sup>-/-</sup> and FVB liver PCTS

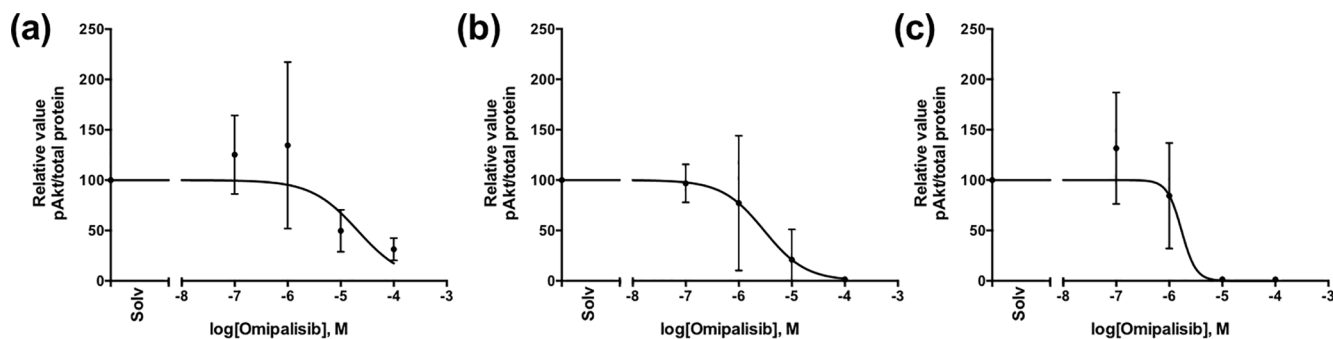


Fig. 3. Ompalisib inhibits Akt phosphorylation in (a) BL/6 mouse, (b) human healthy and (c) human cirrhotic liver PCTS. Liver PCTS were incubated with solvent (Solv) (0.004% DMSO) or increasing concentrations of ompalisib for 1 h; the phosphorylation of Akt was assessed via WB; n = 3.

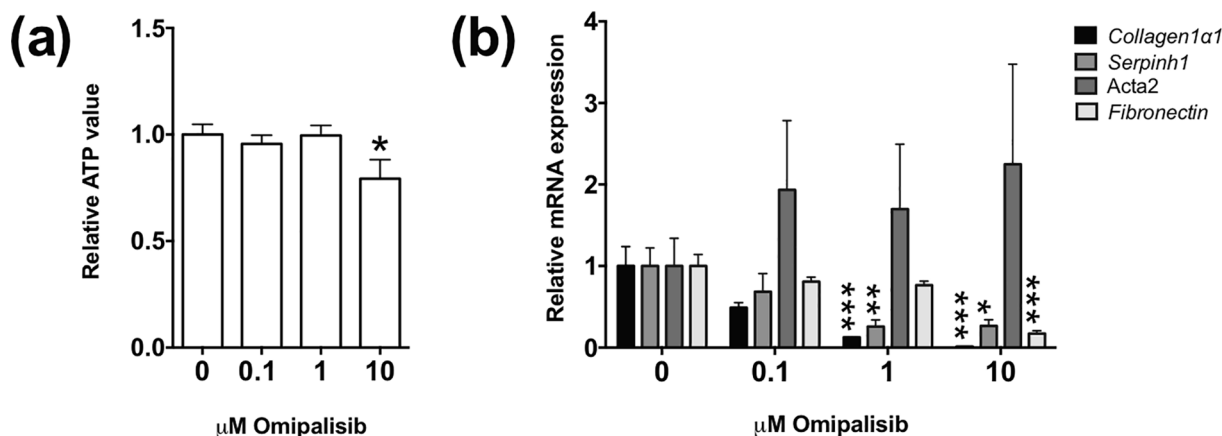


Fig. 4. The effect of ompalisib in BL/6 liver PCTS. (a) Healthy BL/6 PCTS viability during incubation with ompalisib – relative ATP level/protein compared to control (0  $\mu$ M ompalisib); (b) Fibrosis-related gene expression in BL/6 PCTS treated with ompalisib or solvent for 48 h; Data are presented as relative values to 48 h control; n = 6; Data represent mean  $\pm$  SEM; \*p < 0.05, \*\*p < 0.01, \*\*\*p < 0.001 significantly different from control.

(Fig. 5d). The effect of ompalisib on fibrosis marker gene expression in FVB and *Mdr2*<sup>-/-</sup> liver PCTS is shown in Fig. 5c. Expression of *Col1a1* increased during 48 h incubation in both FVB and *Mdr2*<sup>-/-</sup> PCTS, while *Col1a1* expression in FVB PCTS did not reach the gene expression level in *Mdr2*<sup>-/-</sup> directly after slicing. As with BL/6 liver PCTS, *Col1a1* expression was strongly reduced by ompalisib. For FVB liver PCTS, both concentrations of the drug reduced *Col1a1* expression significantly 5 and 30 fold, respectively. Furthermore, 5  $\mu$ M ompalisib reduced *Col1a1* expression to a lower level than that of the control (FVB PCTS 0 h). Moreover, in *Mdr2*<sup>-/-</sup> liver PCTS, both ompalisib concentrations decreased *Col1a1* to lower levels than *Mdr2*<sup>-/-</sup> PCTS at 0 h. *Serpinh1* gene expression showed an increase during incubation only for FVB PCTS. A significant decrease was seen in FVB PCTS with 5  $\mu$ M of the drug, while in *Mdr2*<sup>-/-</sup> PCTS both concentrations reduced *Serpinh1* to a similar level. *Acta2* did not show a significant change during incubation, while 5  $\mu$ M ompalisib reduced its gene expression only in *Mdr2*<sup>-/-</sup> PCTS. *Fn1* expression increased during incubation in both FVB and *Mdr2*<sup>-/-</sup> liver PCTS and ompalisib did not further decrease mRNA levels in any group; in contrast, a significant upregulation of 1.8 times was observed for *Fn1* for *Mdr2*<sup>-/-</sup> PCTS treated with 5  $\mu$ M ompalisib. The results showed good tolerability of the drug in mouse liver PCTS and similar antifibrotic effects when liver PCTS were exposed to 1 or 5  $\mu$ M.

### 3.2.3. CDAA-induced NAFLD PCTS

CDAA-induced NAFLD, where fibrosis is triggered by excess fat accumulation and a mild metabolic deficiency (choline) in the liver, served as second model of murine liver fibrosis. We assessed the effect of PI3K inhibition in steatotic livers with (CDAA) or without (CSAA) liver fibrosis using 1  $\mu$ M ompalisib, in view of the prior *Mdr2*<sup>-/-</sup>

results. CSAA induced simple liver steatosis in BL/6 mice, whereas CDAA induced liver steatohepatitis and fibrosis (Fig. 6a,b) coupled with increased gene expression of fibrosis markers (Fig. 6c). The CDAA diet significantly increased the gene expression of all tested fibrosis markers in comparison to the CSAA diet, especially *Col1a1* (30-fold). During liver PCTS incubation, the tested concentration of 1  $\mu$ M ompalisib did not affect the ATP content of CSAA or CDAA liver PCTS compared to their control (Fig. 6d). During the 48 h incubation *Col1a1*, *Serpinh1* and *Fn1* increased significantly in both CDAA and CSAA PCTS, while *Acta2* showed an increase only in CDAA PCTS. Ompalisib at 1  $\mu$ M reduced *Col1a1* and *Serpinh1* gene expression in CSAA liver PCTS, and *Serpinh1* and *Fn1* in CDAA liver PCTS, with a trend of reduction for *Col1a1* (p = 0.059) (Fig. 6c). The results show that the drug has a good tolerability, but a diminished antifibrotic effect in liver fibrosis triggered by steatosis/steatohepatitis.

### 3.2.4. Healthy human liver PCTS

Next, we assessed if a similar effect of ompalisib would be found for human liver PCTS. The possibility of using human tissue for compound testing is a great advantage of the PCTS method, serving as a bridge between murine and human drug testing for efficacy and side effects, before a clinical study may be initiated. As a model for early onset of fibrosis, we used healthy human liver PCTS [37,39]. Four ompalisib concentrations were tested: 0.1, 1, 5 and 10  $\mu$ M. The two lower concentrations showed no reduction of viability (ATP content, Fig. 7a), but from 5  $\mu$ M on, the decrease in ATP content became significant (5  $\mu$ M – 38% and 10  $\mu$ M – 49% compared to controls). On the gene expression level, healthy human liver PCTS showed a higher variation for fibrosis marker expression than murine PCTS (Fig. 7b). Nonetheless, there was a trend of low ompalisib concentrations (0.1 and 1  $\mu$ M) to lower the

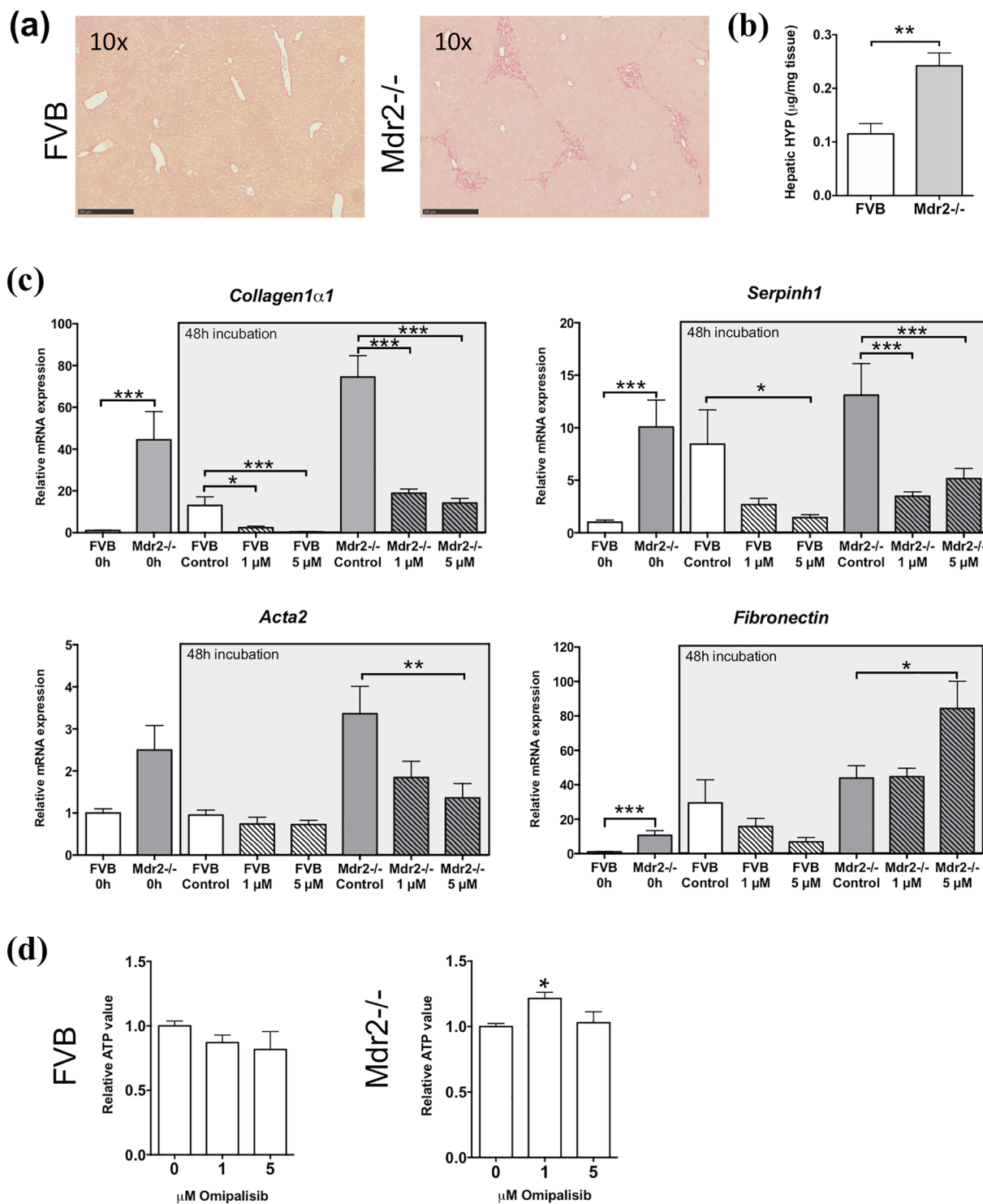


**Fig. 5.** Spontaneous biliary fibrosis in Mdr2<sup>-/-</sup> mice and the effect of omipalisib in FVB and Mdr2<sup>-/-</sup> liver PCTS. (a) Sirius Red staining of representative FVB and Mdr2<sup>-/-</sup> liver PCTS sections at 0 h (no incubation) with 10× magnification. (b) HYP content from FVB and Mdr2<sup>-/-</sup> livers. (c) Fibrosis-related gene expression in FVB and Mdr2<sup>-/-</sup> liver PCTS treated with omipalisib or solvent, data are presented as relative values to FVB 0 h PCLS. (d) Relative ATP level/protein of FVB and Mdr2<sup>-/-</sup> liver PCTS; Data represent mean ± SEM; \*p < 0.05, \*\*p < 0.01, \*\*\*p < 0.001 significantly different from control; n = 6–10. (For interpretation of the references to colour in this figure legend, the reader is referred to the web version of this article.)

gene expression of *COL1a1* and *SERPINH1*. Significant results were obtained only with 5 µM (*COL1a1*, *SERPINH1* transcript reduction by 97% and 70%, respectively) and 10 µM omipalisib (*COL1a1* transcript reduction by 98%). We measured the protein concentration of Pro-Collagen I α1 in the incubation media to determine if the production of collagen is reduced by omipalisib. All tested concentrations of the drug

reduced significantly the concentration of this protein in the media (Fig. 7c); moreover, the decrease was stronger with higher concentrations, going from 70% (0.1 µM) to 85% decrease (10 µM). The results show that the viability of human liver PCTS is more sensitive to PI3K inhibition than mouse liver PCTS, and that the antifibrotic effect on PCR markers is observed only at higher concentrations, while Pro-

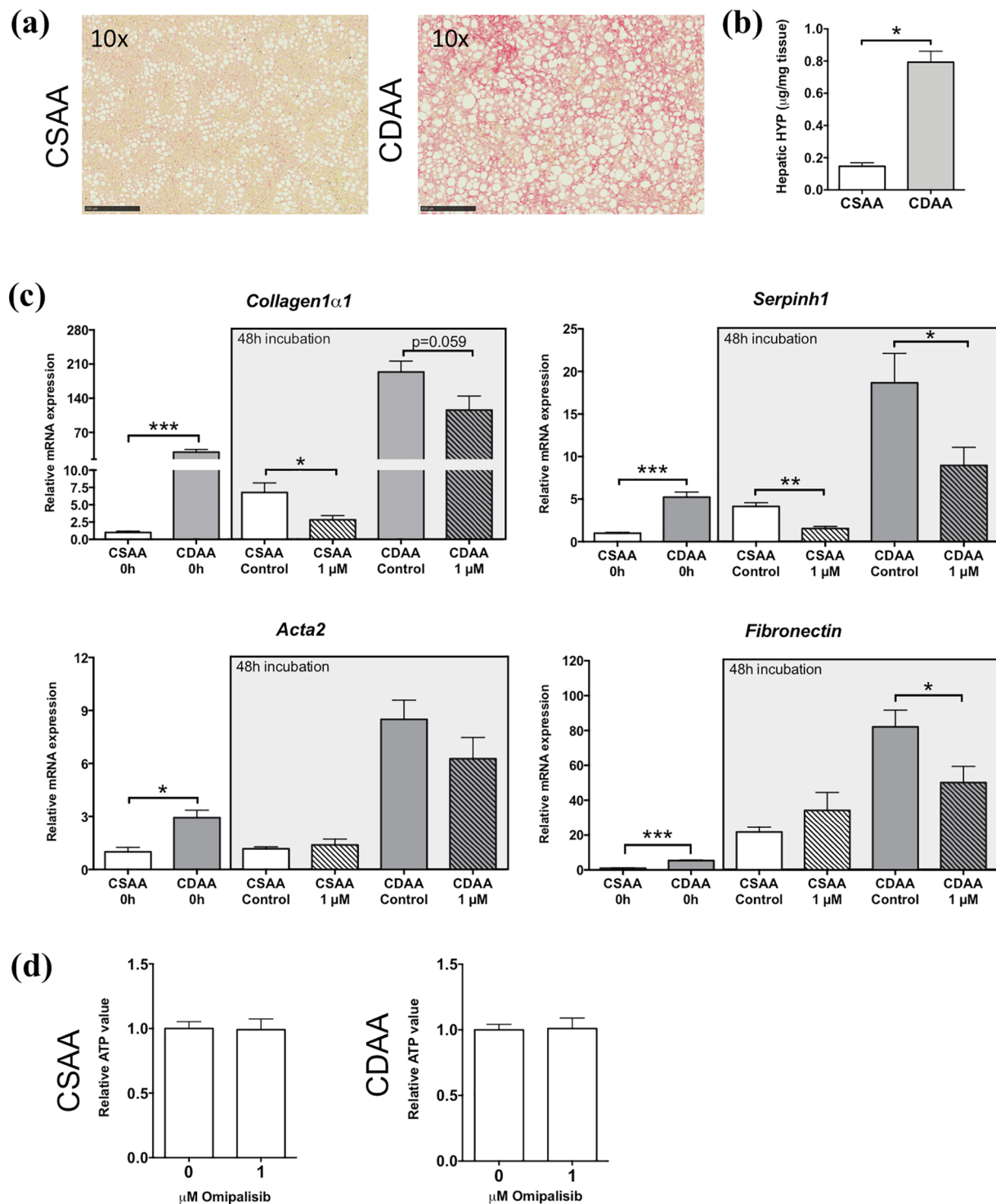


**Fig. 6.** Fibrosis and steatosis in CDAA fed mice and the effect of omipalisib in CSAA and CDAA liver PCTS. (a) Sirius Red staining of representative CSAA and CDAA liver PCTS sections at 0 h (no incubation) with 10× magnification. (b) HYP content for CSAA and CDAA livers. (c) Fibrosis-related gene expression in CSAA and CDAA liver PCTS treated with omipalisib or solvent, data are presented as relative values to CSAA 0 h PCLS. (d) Relative ATP level/protein of CSAA and CDAA liver PCTS; Data represent mean ± SEM; \* $p < 0.05$ , \*\* $p < 0.01$ , \*\*\* $p < 0.001$  significantly different from control;  $n = 4-5$ . (For interpretation of the references to colour in this figure legend, the reader is referred to the web version of this article.)

Collagen I  $\alpha 1$  is reduced by all tested concentrations.

### 3.2.5. Cirrhotic human liver PCTS

To investigate if omipalisib could reduce fibrosis in end-stage liver disease, fibrotic human liver PCTS, as a model for end-stage of fibrosis [21], were incubated with the same concentrations of omipalisib as healthy liver. The difference between healthy and cirrhotic human liver

PCTS regarding SR staining is presented in Fig. 8a, together with the gene expression of the investigated markers (*COL1a1*, *ACTA2*, *SERPINH1*, *FN1*) (Fig. 8b), and the concentration of Pro-Collagen I  $\alpha 1$  secreted during culture (Fig. 8c).

In fibrotic liver PCTS, omipalisib was more toxic compared to mouse and healthy human tissue, as evidenced by the lower ATP content (Fig. 7d) that decreased similarly (by 45%) with 1 and 5 µM compared



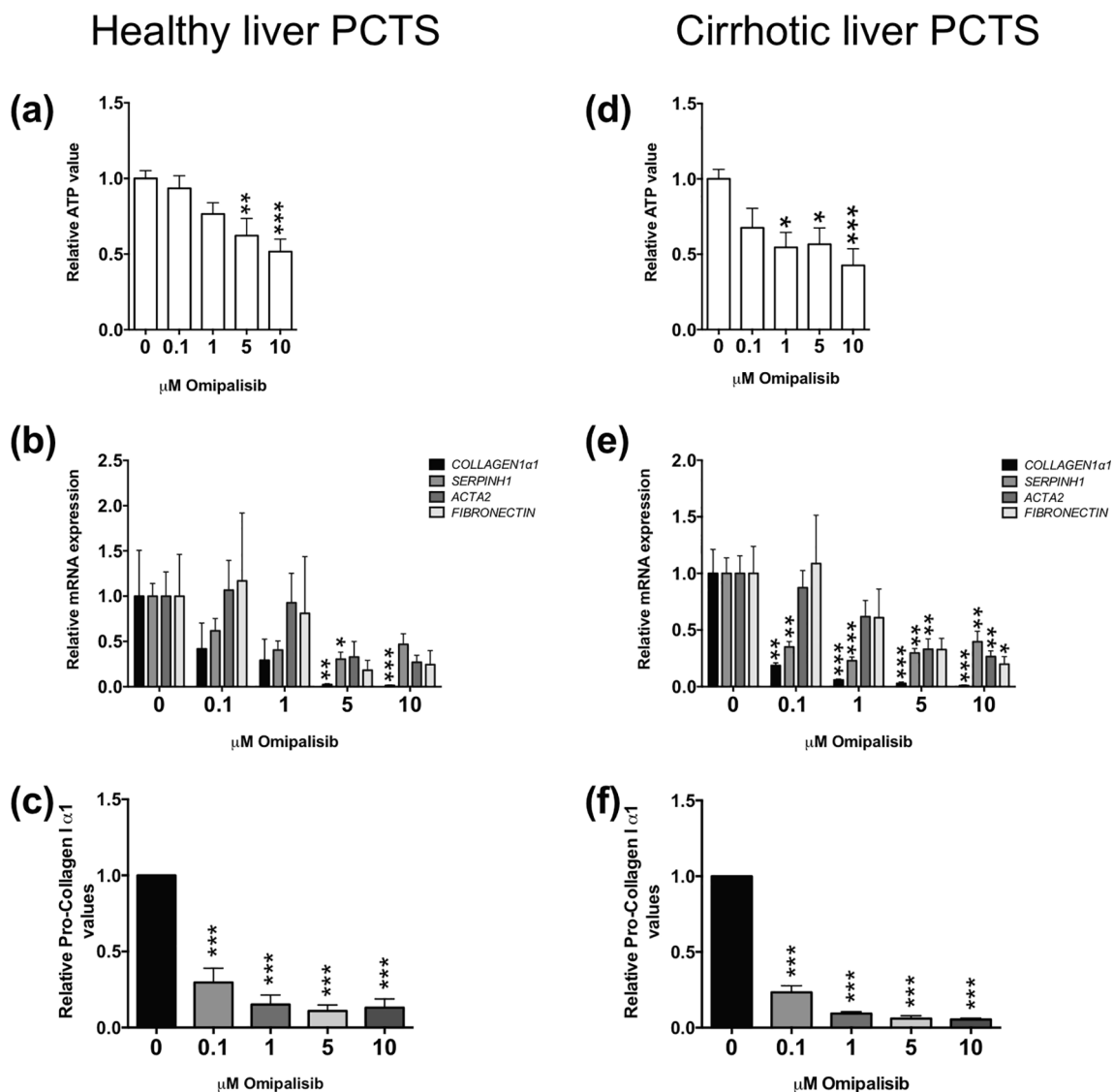


**Fig. 7.** The effect of omipalisib in human liver PCTS. Human liver PCTS viability during incubation with omipalisib or solvent – ATP level/protein in (a) healthy and (b) cirrhotic. Fibrosis-related gene expression in human liver PCTS treated with omipalisib or solvent: (c) healthy and (d) cirrhotic. Pro-Collagen I α1 released by (e) healthy and (f) cirrhotic liver PCTS in culture media during 48 h treatment with omipalisib or solvent. Data presented as means ± SEM; n = 4–5; \*p < 0.05, \*\*p < 0.01, \*\*\*p < 0.001 significantly different from 0 μM omipalisib.

to control, and down by 57% at 10 μM). Notably, on the transcript level, omipalisib strongly reduced *COL1a1* and *SERPINH1*, starting with the lowest tested concentration (Fig. 7e). At 0.1 μM, the reduction of *COL1a1* was 80%, to reach 99% at 10 μM. Only a trend of suppression was found for *ACTA2* and *FN1*, which became significant at 5 μM (*ACTA2*) and 10 μM (*FN1*). Regarding the protein levels of Pro-Collagen I α1 produced and secreted during culture, omipalisib treatment decreased it for all tested concentration (Fig. 7f). At 0.1 μM, the decrease was 75%, whereas the other concentration led to a decrease higher than 90%. The results show that diseased human liver tissue is more susceptible to untoward side effects than healthy liver when exposed to omipalisib, but that the antifibrotic effect was stronger on PCR, being observed already at 0.1 μM omipalisib, and similar for the protein concentration of Pro-Collagen I α1.

### 3.2.6. Omipalisib shows strong toxicity in murine and human jejunum PCTS

Since omipalisib can be administered orally to patients, we assess the effects of this drug on the intestine, since intestinal side effects were reported [24]. We tested omipalisib on murine and human jejunum PCTS. First, similar to our experiments in liver, when we tested 0.1, 1

and 10 μM omipalisib in murine and human jejunum PCTS, there was a dose dependent reduction of ATP content (Fig. 9a, b), with a higher sensitivity of jejunum vs. liver PCTS. We therefore tested a lower concentration: 0.01 μM. This concentration had no toxic effect on mouse jejunum PCTS, but still compromised ATP content of human jejunum PCTS (43% decrease compared to control). We further tested the effect of the non-toxic concentration of omipalisib on the gene expression of fibrosis markers in mouse jejunum PCTS (Fig. 9c). *Colla1* was the only marker that was decreased after 48 h incubation. With regard to the human tissue, we evaluated the morphological changes induced by 0.01 μM omipalisib (Fig. 9d). We observed more necrosis and cellular damage in the sections from PCTS treated with omipalisib. Moreover, the crypts were damaged, the villi were flattened and massive necrosis was noticeable. All together, these results show organ (liver vs. jejunum) and species (mouse-human) differences. They also demonstrate that the human PCTS could predict complications that have been found in human studies.



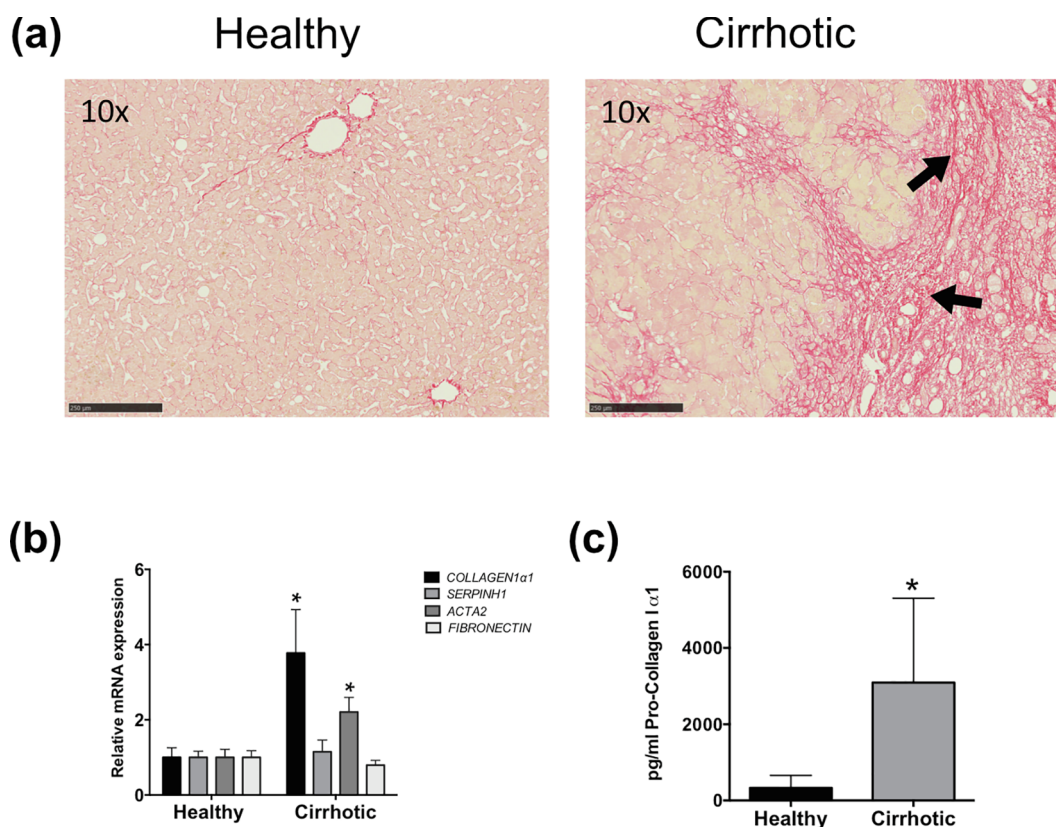


**Fig. 8.** Fibrosis in human liver PCTS. (a) Sirius Red staining of representative healthy and cirrhotic human liver PCTS sections at 0 h (no incubation) with 10 $\times$  magnification; the cirrhotic liver presents excessive extracellular matrix (black arrow). (b) Fibrosis-related gene expression in human healthy and cirrhotic liver PCTS 0 h (no incubation). (c) Pro-Collagen I  $\alpha$ 1 released in the culture media after 48 h incubation of healthy and cirrhotic liver PCTS.  $n = 4-5$ ; data presented as means  $\pm$  SEM; \* $p < 0.05$ , significantly different from healthy liver PCTS. (For interpretation of the references to colour in this figure legend, the reader is referred to the web version of this article.)

#### 4. Discussion

Drug development, a decade-long process, can be facilitated by preclinical studies performed in a complex system that maintains organ structure and reflects cell–cell interactions. In this study, we demonstrated the antifibrotic effect and toxicity of omipalisib, a PI3K pan-inhibitor, in a murine and human *ex vivo* model (PCTS), mimicking early-onset and end-stage liver fibrosis and normal intestine.

The PI3K pathway is essential for cell activation, proliferation, differentiation and survival due to its central role in cell metabolism [12]. Increased PI3K activity is associated with hyperproliferation and cancer [15], thus, PI3K *pan-inhibitors* were developed as chemotherapy [13]. Although omipalisib was initially tested for oncology, Mercer *et al.* studied its antifibrotic effect in human idiopathic pulmonary fibrosis (IPF) PCTS [23], where 0.1  $\mu$ M omipalisib decreased collagen formation. We showed that similar concentrations are necessary in liver PCTS and that these values are 2–3 orders of magnitude higher than the concentrations needed in cell-free assays (picomolar range [18]). We showed species and organ differences regarding drug toxicity. Species differences are shown by the higher viability (absolute values of ATP/ $\mu$ g protein) of murine PCTS treated with omipalisib than human PCTS. Additionally, 10  $\mu$ M omipalisib induced a 20% decrease in viability in healthy BL/6 liver PCTS, while the viability of healthy human liver PCTS was reduced by 50%. This can be explained by the fact that murine liver PCTS have a higher IC<sub>50</sub> value than human liver PCTS (Fig. 3). Another factor that can contribute to this difference is tissue quality – mouse liver is excised directly after sacrifice, whereas the human tissue goes through warm ischemia due to surgical protocol. We illustrated similar species differences in jejunum PCTS. Further, we showed organ differences regarding PI3K inhibition between liver and

jejunum in both species. The concentrations tested in liver PCTS were toxic for jejunum PCTS, confirming the high intestinal sensitivity to PI3K inhibition. These results are in line with *in vivo* data from oncologic patients who received PI3K inhibitors [8] and IPF patients treated with omipalisib in phase I clinical trial, who often presented gastrointestinal problems, such as diarrhea [4,6,22]. This is a mechanism-related side effect and can be explained by the prime role of the small intestine in nutrient sensing and uptake, and by its high turnover of intestinal epithelial cells. PI3K inhibition in intestinal Caco-2/15 affects E-cadherin – a cell adhesion molecule, involved in maintaining intestinal barrier integrity [19]. Given these points, and considering that the class of PI3K inhibitors is administered orally, the formulation should be improved or another pharmaceutical form than oral should be developed. Last, we want to draw attention on disease-related differences that influence PI3K inhibition toxicity. Viability decrease by 40% starting from 5  $\mu$ M omipalisib for healthy human liver slices, whereas a higher decrease in viability (45%) was observed in cirrhotic liver PCTS already at 1  $\mu$ M. Still, 30–50% decrease in viability is considered medium toxicity [36]. The only concentration that affected viability with more than 50% was 10  $\mu$ M omipalisib in human cirrhotic liver PCTS, showing higher toxic effects for late stage disease. Altogether, omipalisib shows more toxicity in human than murine PCTS and jejunum is more sensitive to PI3K inhibition than liver.

Assessing the antifibrotic effect of omipalisib in liver PCTS was another goal. We used the model for early onset of fibrosis – murine and human healthy liver. Omipalisib showed an antifibrotic effect on healthy BL/6 liver PCTS already at 1  $\mu$ M by reducing the expression of the key ECM genes *Col1a1* and *Fn1*. However, myofibroblast activation (assessed by *Acta2*) did not respond to omipalisib treatment. Healthy human liver PCTS responded to omipalisib treatment by reducing the

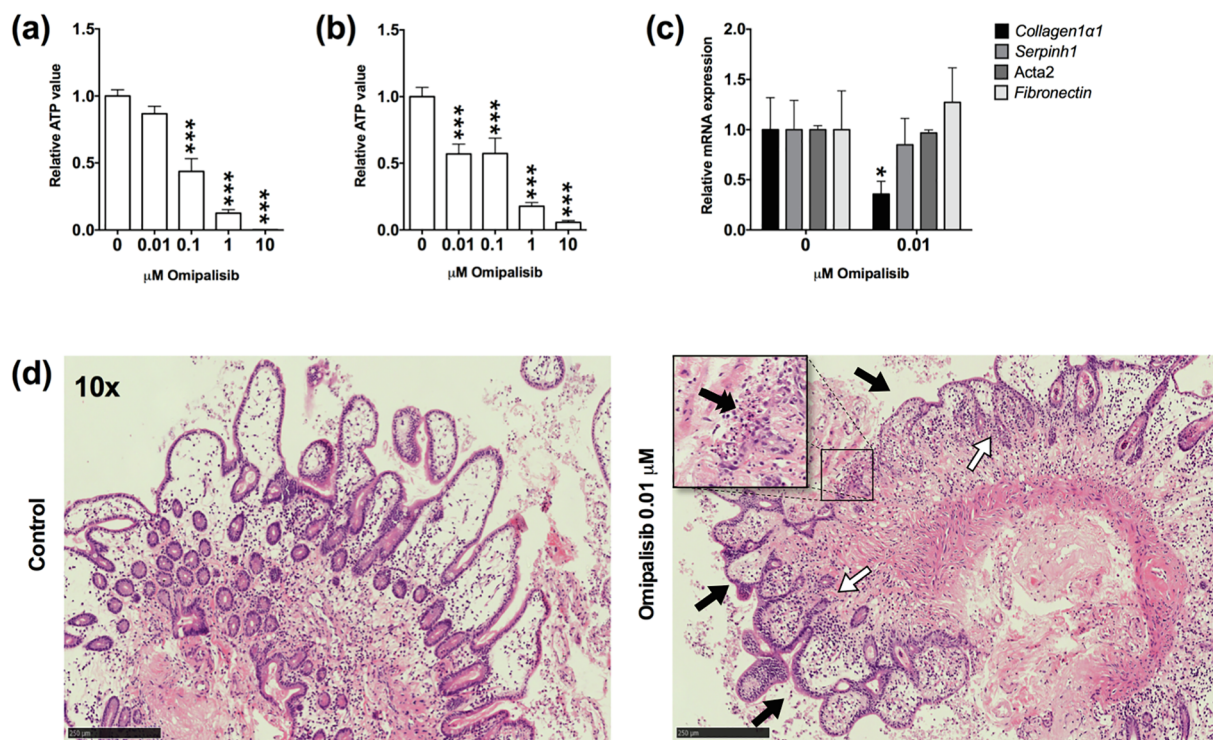


**Fig. 9.** The effect of omipalisib on jejunum PCTS – ATP level/protein: (a) BL/6 healthy jejunum PCTS (n = 3–9), (b) human healthy jejunum PCTS (n = 3–5). (c) Fibrosis-related gene expression in PCTS BL/6 healthy jejunum PCTS treated with omipalisib or solvent (n = 5). Data presented as means  $\pm$  SEM; \*p < 0.05, \*\*\*p < 0.001 different from 0  $\mu\text{M}$  omipalisib. (d) Representative H&E staining of human jejunum PCTS treated with omipalisib 0.01  $\mu\text{M}$  or solvent (control), 10  $\times$  magnification; the sample treated with omipalisib showed flattened villi (black arrow), damaged crypts (empty arrow) and necrosis (two-headed arrow).

protein expression of Pro-Collagen I  $\alpha$ 1, but showed a high variation for the analyzed markers on PCR. This can be explained by the above-discussed high patient inter-individual differences. Although all human tissues are considered clinically healthy, patients might have been exposed to alcohol, medication or toxins that might cause the observed differences in fibrogenic activation. Similarly to mouse liver PCTS, myofibroblast activation was not affected. Thus, omipalisib has an antifibrotic effect in healthy murine and human liver PCTS that appears independent of the myofibroblast activation marker ACTA2.

An important part of this investigation was to evaluate the antifibrotic efficacy of omipalisib in fibrotic liver PCTS. The end-stage model of fibrosis allowed us to test omipalisib in chronically damaged PCTS with an enhanced baseline level of and higher *in vitro* susceptibility to fibrogenic activation. Mouse experiments included two models of liver fibrosis, with different etiologies: spontaneous biliary fibrosis in *Mdr2*<sup>-/-</sup> mice resembling human primary sclerosing cholangitis [11], mere fatty liver (CSAA) and steatohepatitis with fibrosis (CDA) [10]. *Ex vivo* incubation triggered additional fibrosis in these PCTS. We observed a stronger fibrosis induction during culture in CDA than in *Mdr2*<sup>-/-</sup> PCTS and this could be explained by the fact that the CDA diet induces steatosis and inflammation [40], which might have a synergistic effect on increasing fibrosis markers during culture. The antifibrotic effect of omipalisib was similar in these two models, though stronger in *Mdr2*<sup>-/-</sup> PCTS. An unexpected result was the increased expression of *Fn1* caused by 5  $\mu\text{M}$  omipalisib in the *Mdr2*<sup>-/-</sup> PCTS. As fibronectin is involved in cell adhesion, differentiation and migration [5,16], our results might indicate that a high concentration of omipalisib in *Mdr2*<sup>-/-</sup> fibrotic liver could trigger one of these pathway, resulting in increased *Fn1* expression. In CDA PCTS we observed a limited antifibrotic effect that can be related to omipalisib's lipophilicity (partition coefficient – 3.3 [17]); this could lead to a different intracellular concentration as a result of altered transporters and hepatic metabolism in NAFLD [7,25]. The metabolism of omipalisib is not reported in literature. This shows that the pharmacokinetic properties

can be affected by steatosis [25]. Therefore, the effects of PI3K inhibition on inflammation, oxidative stress and lipid metabolism need to be assessed. Next, in diseased human liver PCTS we observed less variability than in healthy human liver, and the antifibrotic effect of omipalisib was achieved already at 0.1  $\mu\text{M}$ . This shows that the drug is more efficient in end-stage than early fibrosis, since the concentration needed to achieve a significant reduction of *COL1 $\alpha$ 1* was 50 times lower. An explanation can be the elevated level of this key fibrogenic gene prior incubation in diseased compared to healthy liver (4-fold higher) and the fact that compared to healthy PCTS, slices from cirrhotic liver produce more Pro-Collagen I  $\alpha$ 1 during culture (Fig. 8c). Interestingly, the gene expression of myofibroblast activation marker – ACTA2, was reduced by omipalisib only in end-stage models of fibrosis (*Mdr2*<sup>-/-</sup> and cirrhotic liver PCTS) at high concentrations, suggesting differences for markers' sensitivity to the drug. Overall, omipalisib shows a clear antifibrotic effect in diseased murine and human livers, showing the importance of PI3K pathway in ECM production.

The method of PCTS for preclinical drug testing is highly useful due to several advantages: 1) preservation of the 3D structure and cellular organization, 2) reproducibility, 3) possibility to test the human system, 4) possibility to test different drug concentrations in the same tissue prepared and cultured under the same conditions, 5) exploration of drug effects during early onset and end-stage fibrosis, 6) detection of adverse events due to drug toxicity and pharmacokinetic studies in the target but also other organs. However, the method also has disadvantages: 1) limitation to short term incubation due to PCTS decrease of viability after 48 h of incubation [9], 2) major effects being observed on the gene expression level, while changes on the level of protein expression of morphology are often limited, 3) a lack of blood derived immune cells. Nonetheless, even if imperfect, the advantages of the methodology surpass the disadvantages and we are confident that ongoing validation and comparison with *in vivo* data will further confirm PCTS as a valuable tool for preclinical studies of fibrosis and organ toxicity. Importantly, our preclinical testing of omipalisib in murine



PCTS would predict that omipalisib would not be a good candidate for the treatment of NASH-induced fibrosis as compared to biliary fibrosis, for the above-mentioned reasons.

At present, liver fibrosis is a progressive condition incurring a high morbidity and mortality, with no specific treatment. ECM production has a central role in wound healing, but its excessive production in “wounds that do not heal” will lead to remodeling of the organ, architecture and final loss of organ function. To prevent the vicious cycle of ECM accumulation and increasing matrix stiffness that further drives inflammation and fibrosis [29], a drug that can attenuate the exaggerated ECM production and thus interrupt this vicious cycle is needed. The current study shows positive results achieved through PI3K pathway inhibition, specifically the decrease of fibrosis markers. However, this ubiquitous pathway is involved in many cellular processes, making its inhibition a double-edged sword. The sensitivity of the gastro-intestinal tract poses a central problem to high dose systemic PI3K pan-inhibitor therapy. For these reasons, cell targeting towards the organ of interest and the ECM producing cells by specific drug formulations to protect the gastro-intestinal tract are needed.

### Declaration of Competing Interest

A. Oldenburger and J.F. Rippmann are employees at Boehringer Ingelheim Pharma GmbH & Co. KG.

### Acknowledgements

This research was supported by ZonMw (the Netherlands Organisation for Health Research and Development), grant number 114025003.

DS receives project related support by the EU Horizon 2020 under grant agreement n. 634413 (EPoS, European Project on Steatohepatitis) and 777377 (LITMUS, Liver Investigation on Marker Utility in Steatohepatitis), and by the German Research Foundation collaborative research project grants DFG CRC 1066/B3 and CRC 1292/08.

We would like to thank the group of Dr. Andre Broermann from the Cardiometabolic Disease Research group at Boehringer Ingelheim Pharma GmbH & Co. KG for providing us with the mice on the CDA and CSAA diets.

### References

- [1] P. Angulo, Nonalcoholic fatty liver disease, *N. Engl. J. Med.* 346 (2002) 1221–1231, <https://doi.org/10.1056/NEJMra011775>.
- [2] E. Banham-Hall, M.R. Clatworthy, K. Okkenhaug, The therapeutic potential for PI3K inhibitors in autoimmune rheumatic diseases, *Open Rheumatol. J.* 6 (2012) 245–258, <https://doi.org/10.2174/1874312901206010245>.
- [3] R. Bataller, D.A. Brenner, Liver fibrosis, *J. Clin. Invest.* 115 (2005) 209–218, <https://doi.org/10.1172/JCI200524282>.
- [4] C.Y. Cheah, L.J. Nastoupil, S.S. Neelapu, S.G. Forbes, Y. Oki, N.H. Fowler, Lenalidomide, idelalisib, and rituximab are unacceptably toxic in patients with relapsed/refractory indolent lymphoma, *Blood* 125 (2015) 3357–3359, <https://doi.org/10.1182/blood-2015-03-633156>.
- [5] W. Chen, L.A. Culp, Adhesion mediated by fibronectin's alternatively spliced EDb (EIIIB) and its neighboring type III repeats, *Exp. Cell Res.* 223 (1996) 9–19, <https://doi.org/10.1006/excr.1996.0053>.
- [6] S. Chia, S. Gandhi, A.A. Joy, S. Edwards, M. Gorr, S. Hopkins, J. Kondejewski, J.P. Ayoub, N. Califaretti, D. Rayson, S.F. Dent, Novel agents and associated toxicities of inhibitors of the pi3k/Akt/mTOR pathway for the treatment of breast cancer, *Curr. Oncol.* 22 (2015) 33–48, <https://doi.org/10.3747/co.22.2393>.
- [7] X. Chu, K. Korzekwa, R. Elsby, K. Fenner, A. Galetin, Y. Lai, P. Mattsson, A. Moss, S. Nagar, G.R. Rosania, J.P.F. Bai, J.W. Polli, Y. Sugiyama, K.L.R. Brouwer, Intracellular drug concentrations and transporters: measurement, modeling, and implications for the liver, *Clin. Pharmacol. Ther.* 94 (2013) 126–141, <https://doi.org/10.1038/clpt.2013.78>.
- [8] S.E. Coutre, J.C. Barrientos, J.R. Brown, S. de Vos, R.R. Furman, M.J. Keating, D. Li, S.M. O'Brien, J.M. Pagel, M.H. Poleski, J.P. Sharman, N.-S. Yao, A.D. Zelenetz, Management of adverse events associated with idelalisib treatment – expert panel opinion, *Leuk. Lymphoma* 8194 (2015) 1–20, <https://doi.org/10.3109/10428194.2015.1022770>.
- [9] I.A.M. de Graaf, P. Olinga, M.H. de Jager, M.T. Merema, R. de Kanter, E.G. van de Kerkhof, G.M.M. Groothuis, Preparation and incubation of precision-cut liver and intestinal slices for application in drug metabolism and toxicity studies, *Nat. Protoc.* 5 (2010) 1540–1551, <https://doi.org/10.1038/nprot.2010.111>.
- [10] G. Farrell, J.M. Schattenberg, I. Leclercq, M.M. Yeh, R. Goldin, N. Teoh, D. Schuppan, Mouse models of nonalcoholic steatohepatitis Towards optimization of their relevance to human NASH, *Hepatology* 2 (2018), <https://doi.org/10.1002/hep.30333>.
- [11] P. Fickert, A. Fuchsichler, M. Wagner, G. Zollner, A. Kaser, H. Tilg, R. Krause, F. Lammert, C. Langner, K. Zatlouk, H.U. Marschall, H. Denk, M. Trauner, Regurgitation of bile acids from leaky bile ducts causes sclerosing cholangitis in Mdr2 (Abcb4) knockout mice, *Gastroenterology* 127 (2004) 261–274, <https://doi.org/10.1053/j.gastro.2004.04.009>.
- [12] A. Fort, N. Calo, D. Portius, L. Bourgoign, M. Peyrou, M. Foti, *Signaling Pathways in Liver Diseases*, John Wiley & Sons Ltd, Chichester, UK, 2015 Doi: 10.1002/9781118663387.
- [13] L.C. Foukas, I.M. Berenjeno, A. Gray, A. Khwaja, B. Vanhaesebroeck, Activity of any class IA PI3K isoform can sustain cell proliferation and survival, *Proc. Natl. Acad. Sci.* 107 (2010) 11381–11386, <https://doi.org/10.1073/pnas.0906461107>.
- [14] D.A. Fruman, R.E. Meyers, L.C. Cantley, Phosphoinositide kinases, *Annu. Rev. Biochem.* 67 (1998) 481–507, <https://doi.org/10.1146/annurev.biochem.67.1.481>.
- [15] D.A. Fruman, C. Rommel, PI3K and cancer: lessons, challenges and opportunities, *Nat. Rev. Drug Discov.* 13 (2014) 140–156, <https://doi.org/10.1038/nrd4204>.
- [16] T. Fukuda, N. Yoshida, Y. Kataoka, R. Manabe, Y. Mizuno-Horikawa, M. Sato, K. Kuriyama, N. Yasui, K. Sekiguchi, Mice lacking the EDB segment of fibronectin develop normally but exhibit reduced cell growth and fibronectin matrix assembly in vitro, *Cancer Res.* 62 (2002) 5603–5610, <https://pubchem.ncbi.nlm.nih.gov/compound/gsk2126458#section=Top>.
- [17] S.D. Knight, N.D. Adams, J.L. Burgess, A.M. Chaudhari, M.G. Darcy, C.A. Donatelli, J.I. Luengo, K.A. Newlander, C.A. Parrish, L.H. Ridgers, M.A. Sarpong, S.J. Schmidt, G.S. Van Aller, J.D. Carson, M.A. Diamond, P.A. Elkins, C.M. Gardiner, E. Garver, S.A. Gilbert, R.R. Gontarek, J.R. Jackson, K.L. Kershner, L. Luo, K. Raha, C.S. Sherk, C.-M. Sung, D. Sutton, P.J. Tummino, R.J. Wegrzyn, K.R. Auger, D. Dhanak, Discovery of GSK2126458, a Highly Potent Inhibitor of PI3K and the Mammalian Target of Rapamycin, *ACS Med. Chem. Lett.* 1 (2010) 39–43, <https://doi.org/10.1021/ml900028r>.
- [18] P. Laprise, P. Chailier, M. Houde, J.-F. Beaulieu, M.-J. Boucher, N. Rivard, Phosphatidylinositol 3-kinase controls human intestinal epithelial cell differentiation by promoting adherens junction assembly and p38 MAPK activation, *J. Biol. Chem.* 277 (2002) 8226–8234, <https://doi.org/10.1074/jbc.M110235200>.
- [19] D. Li, L. He, H. Guo, H. Chen, H. Shan, Targeting activated hepatic stellate cells (aHSCs) for liver fibrosis imaging, *EJNMMI Res.* 5 (2015) 71, <https://doi.org/10.1186/s13550-015-0151-x>.
- [20] T. Luangmonkong, S. Suriguga, E. Bigaeva, M. Boersema, D. Oosterhuis, K.P. de Jong, D. Schuppan, H.A.M. Mutsaers, P. Olinga, Evaluating the antifibrotic potency of galunisertib in a human ex vivo model of liver fibrosis, *Br. J. Pharmacol.* 174 (2017) 3107–3117, <https://doi.org/10.1111/bph.13945>.
- [21] P.T. Lukey, S.A. Harrison, S. Yang, Y. Man, B.F. Holman, A. Rashidnasab, G. Azzopardi, M. Grayer, J.K. Simpson, P. Bareille, L. Paul, H.V. Woodcock, R. Toshner, P. Saunders, P.L. Molyneaux, K. Thielemans, F.J. Wilson, P.F. Mercer, R.C. Chambers, A.M. Groves, W.A. Fahy, R.P. Marshall, T.M. Maher, A randomised, placebo-controlled study of omipalisib (PI3K/mTOR) in idiopathic pulmonary fibrosis, *Eur. Respir. J.* 53 (2019) 1801992, <https://doi.org/10.1183/13993003.01992-2018>.
- [22] P.F. Mercer, H.V. Woodcock, J.D. Eley, M. Platé, M.G. Sulikowski, P.F. Durrenberger, L. Franklin, C.B. Nanthakumar, Y. Man, F. Genovese, R.J. McAnulty, S. Yang, T.M. Maher, A.G. Nicholson, A.D. Blanchard, R.P. Marshall, P.T. Lukey, R.C. Chambers, Exploration of a potent PI3 kinase/mTOR inhibitor as a novel anti-fibrotic agent in IPF, *Thorax* 71 (2016) 710–711, <https://doi.org/10.1136/thoraxjnl-2015-207429>.
- [23] P. Munster, R. Aggarwal, D. Hong, J.H.M. Schellens, R. van der Noll, J. Specht, P.O. Witteveen, T.L. Werner, E.C. Dees, E. Bergsland, N. Agarwal, J.F. Kleha, M. Durante, L. Adams, D.A. Smith, T.A. Lampkin, S.R. Morris, R. Kurzrock, First-in-human phase I study of GSK2126458, an oral pan-class I phosphatidylinositol-3-kinase inhibitor, in patients with advanced solid tumor malignancies, *Clin. Cancer Res.* 22 (2016) 1932–1939, <https://doi.org/10.1158/1078-0432.CCR-15-1665>.
- [24] A. Naik, A. Belić, U.M. Zanger, D. Rozman, Molecular Interactions between NAFLD and Xenobiotic Metabolism, *Front. Genet.* 4 (2013) 1–14, <https://doi.org/10.3389/fgene.2013.00002>.
- [25] Y. Popov, E. Patsenker, P. Fickert, M. Trauner, D. Schuppan, Mdr2 (Abcb4) – /– mice spontaneously develop severe biliary fibrosis via massive dysregulation of pro- and antifibrogenic genes, *J. Hepatol.* 43 (2005) 1045–1054, <https://doi.org/10.1016/j.jhep.2005.06.025>.
- [26] Y. Popov, E. Patsenker, F. Stickle, J. Zaks, K.R. Bhaskar, G. Niedobitek, A. Kolb, H. Friess, D. Schuppan, Integrin  $\alpha v \beta 6$  is a marker of the progression of biliary and portal liver fibrosis and a novel target for antifibrotic therapies, *J. Hepatol.* 48 (2008) 453–464, <https://doi.org/10.1016/j.jhep.2007.11.021>.
- [27] D. Schuppan, N.H. Afdhal, Liver cirrhosis, *Lancet* 371 (2008) 838–851, [https://doi.org/10.1016/S0140-6736\(08\)60383-9](https://doi.org/10.1016/S0140-6736(08)60383-9).
- [28] D. Schuppan, M. Ashfaq-Khan, A.T. Yang, Y.O. Kim, Liver fibrosis: Direct anti-fibrotic agents and targeted therapies, *Matrix Biol.* 68–69 (2018) 435–451, <https://doi.org/10.1016/j.matbio.2018.04.006>.
- [29] D. Schuppan, Y.O. Kim, Evolving therapies for liver fibrosis, *J. Clin. Invest.* 123 (2013) 1887–1901, <https://doi.org/10.1172/JCI66028>.
- [30] D. Schuppan, M. Ruehl, R. Somasundaram, E.G. Hahn, Matrix as a modulator of hepatic fibrogenesis, *Semin. Liver Dis.* 21 (2001) 351–372, <https://doi.org/10.1055/s-2001-17556>.
- [31] D. Schuppan, R. Surabattula, X.Y. Wang, Determinants of fibrosis progression and regression in NASH, *J. Hepatol.* 68 (2018) 238–250, <https://doi.org/10.1016/j.jhep.2018.04.006>.

- [jhep.2017.11.012](https://doi.org/10.1016/j.jhep.2017.11.012).
- [33] M.K. Son, Y.-L. Ryu, K.H. Jung, H. Lee, H.S. Lee, H.H. Yan, H.J. Park, J.-K. Ryu, J.-K. Suh, S. Hong, S.-S. Hong, HS-173, a novel PI3K inhibitor, attenuates the activation of hepatic stellate cells in liver fibrosis, *Sci. Rep.* 3 (2013) 3470, <https://doi.org/10.1038/srep03470>.
- [34] L.M. Thorpe, H. Yuzugullu, J.J. Zhao, PI3K in cancer: divergent roles of isoforms, modes of activation and therapeutic targeting, *Nat. Rev. Cancer* 15 (2015) 7–24, <https://doi.org/10.1038/nrc3860>.
- [35] T. Tsuchida, S.L. Friedman, Mechanisms of hepatic stellate cell activation, *Nat. Rev. Gastroenterol. Hepatol.* 14 (2017) 397–411, <https://doi.org/10.1038/nrgastro.2017.38>.
- [36] S. Vatakuti, J.L.A. Pennings, E. Gore, P. Olinga, G.M.M. Groothuis, Classification of cholestatic and necrotic hepatotoxicants using transcriptomics on human precision-cut liver slices, *Chem. Res. Toxicol.* 29 (2016), <https://doi.org/10.1021/acs.chemrestox.5b00491>.
- [37] I.M. Westra, H.A.M. Mutsaers, T. Luangmonkong, M. Hadi, D. Oosterhuis, K.P. de Jong, G.M.M. Groothuis, P. Olinga, Human precision-cut liver slices as a model to test antifibrotic drugs in the early onset of liver fibrosis, *Toxicol. Vitro* 35 (2016) 77–85, <https://doi.org/10.1016/j.tiv.2016.05.012>.
- [38] I.M. Westra, D. Oosterhuis, G.M.M. Groothuis, P. Olinga, Precision-cut liver slices as a model for the early onset of liver fibrosis to test antifibrotic drugs, *Toxicol. Appl. Pharmacol.* 274 (2014) 328–338, <https://doi.org/10.1016/j.taap.2013.11.017>.
- [39] I.M. Westra, B.T. Pham, G.M.M. Groothuis, P. Olinga, Evaluation of fibrosis in precision-cut tissue slices, *Xenobiotica* 43 (2013) 98–112, <https://doi.org/10.3109/00498254.2012.723151>.
- [40] A. Wree, M.D. McGeough, C.A. Peña, M. Schlattjan, H. Li, M.E. Inzaugarat, K. Messer, A. Canbay, H.M. Hoffman, A.E. Feldstein, NLRP3 inflammasome activation is required for fibrosis development in NAFLD, *J. Mol. Med.* 92 (2014) 1069–1082, <https://doi.org/10.1007/s00109-014-1170-1>.
- [41] J. Yang, J. Nie, X. Ma, Y. Wei, Y. Peng, X. Wei, Targeting PI3K in cancer: mechanisms and advances in clinical trials, *Mol. Cancer* 18 (1) (2019) 26, <https://doi.org/10.1186/s12943-019-0954-x>.